ENCIT 2018

ABCM Associação Brasileira de Engenharia e Ciências Mecânicas

17th Brazilian Congress of Thermal Sciences and Engineering
November 25th-28th, 2018, Águas de Lindóia, SP, Brazil

NUMERICAL INVESTIGATION OF WEAKLY IONISED GAS EFFECTS ON THE SARA CAPSULE

Rodrigo C. Palharini
João Luiz F. Azevedo
Instituto de Aeronáutica e Espaço, DCTA/IAE/ALA, São José dos Campos, SP, 12228-904, Brazil
palharini.rc@gmail.com; joaoluiz.azevedo@gmail.com

Abstract: *In the present work, reactive rarefied gas flows over the SARA capsule were performed using the direct simulation Monte Carlo method. The main goal of this work is to access the influence of weakly ionised gas flows during the SARA reentry phase at 80 km altitude. In order to perform the chemical reactions the Quantum-Kinetic chemistry model was implemented into the dsmcFoam code. According to the results, the chemical reactions have a significant influence on the temperature reduction of the shock wave and flowfield structure surrounding the SARA capsule.*
Keywords: *Aerothermodynamics, Ionised flows, Reentry, DSMC, Rarefied flows*

1. INTRODUCTION

The evaluation of flow structure around a re-entry vehicle has always been one of the key issues in the design of space vehicles. Due to high-energy shock wave formed upstream of these vehicles, free electrons may be produced if the air molecules collisions energy is sufficient. As a result, a weakly ionise gas affects the flowfield structure and may cause a temporary interruption of data transfer between the spacecraft and ground stations. In order to alleviate the blackout problem, it is important to be able to determine the distribution of electrons near the vehicle surface. In this way, an extended version of the Quantum-Kinetic chemistry model has been implemented into the dsmcFoam code and applied in investigation of the Brazilian Reentry Satellite (SARA) during the reentry phase (Mather *et al.*, 2005).

SARA suborbital platform has been developed by the Instituto de Aeronáutica e Espaço at DCTA (Departamento de Ciência e Tecnologia Aeroespacial) in order to conduct scientific and technological experiments in low gravity environment. This capsule can carry up to 55 kg of scientific equipment, stay in orbit during the execution of the experiments, and return to Earth after the accomplishment of the tasks (MCTI-AEB, 2012). For the particular case of SARA capsule, a few studies are available in the current literature and just some of them is discussed below.

Morgenstern and Moraes Jr. (2003) provided a detailed experimental and numerical investigation of the flowfield in the base region of the capsule. It was observed the formation of two main vortices characterized by a unsteady flow region. The effect of this unsteady perturbation on the flowfield in the external cylindrical region, where the parachute pressure sensors are located, was the main concern of this study. The numerical solution showed good agreement with the experimental data and a better understanding on the wake flowfield characteristics was achieved.

Numerical studies of hypersonic blunt body flows with chemical non-equilibrium conditions were investigated by Guzzo and Azevedo (2010). The main objective of their work was to conceive a comprehensive understanding of the Eulerian/Lagrangian hybrid methodology and to test and validate the code over simple configurations. The results showed a good agreement for the overall flow structure and shock wave position when compared with available literature. In addition, the hybrid code seems to be less influenced by the grid parameters and presented a robust approach for hypersonic problems.

Machado (2012) has presented a computational two-dimensional transient aerodynamic investigation of heating and ablation processes on the Brazilian sub-orbital Platform. Considering the capsule composed by two layers, the stainless steel structure and the thermal protection system, this study was able to capture the temperature peak and to represent the ablation process.

Hypersonic non-reacting gas flow simulations over an axisymmetric version of the SARA capsule were conducted by Santos (2013) for altitude varying from 100 to 80 km altitude. The objective of his work was the investigation of the surface accommodation coefficients on the aerodynamic forces acting on the capsule surface, and of the heat transfer rates to the capsule surface.

Palharini and Azevedo (2017) performed rarefied hypersonic gas flow over the SARA capsule in order to investigated the influence of chemical reactions on surface quantities and shock wave structured. It was found that chemical reactions lead to a significant reduction on the shock wave temperature as well as in heat transfer coefficient.

The planetary atmospheres through which hypersonic vehicles may pass consist of a number of chemical species. Although, it is known that the gas in the atmosphere is composed, at microscopic level, of discrete atoms and molecules, a useful approximation arises if the atmosphere is treated as a continuum. The flow over a vehicle moving through the

atmosphere can then be modelled by appealing to the fundamental principles of momentum interchange and mass and energy conservation. This continuum approach is at the root of conventional computational fluid dynamics (CFD) methods for the solution of the Navier-Stokes (NS) equations (Bertin and Cummings, 2006). However, as the Knudsen number increases, the non-continuum, particulate-like behaviour of the gas becomes more important. Numerical models hoping to simulate such rarefied conditions must be able capture the complex physics for high-speed vehicle re-entry. The flow environment is characterised by a distinct bow-shock upstream of the body followed by a high temperature region immediately downstream of the shock. In this searingly hot region, chemical reactions may take place involving dissociation, exchange and ionisation. In the lee side of the craft there is a highly rarefied zone within which thermochemical nonequilibrium conditions may exist. The paucity of molecules in this zone may require that the region be described using a non-continuum, particle-based formulation. In an attempt to further investigate such flow regime, Bird (Bird, 1994) proposed the direct simulation Monte Carlo method (DSMC), which has become the main computational tool for the study of hypersonic aerothermodynamics.

The precise determination of the flowfield structure under thermochemical nonequilibrium conditions is of fundamental importance to mitigate the effects of chemical reactions on space platforms. In this way, the primary goal of the research is to compute inert and reactive gas flows over the SARA capsule at 80 km altitude in order to gain a better understanding of the impact of weakly ionised gas on the flowfield structure surrounding the vehicle.

2. COMPUTATIONAL METHOD

In highly rarefied environments (Kn $>$ 0.1) the analysis of gas flows in the non-continuum regime is most naturally conducted using specialized computational techniques that are derived from a statistical mechanical representation of the behavior of individual particles. The most successful of these techniques is undoubtedly the direct simulation Monte Carlo (DSMC) approach, originally proposed by Bird (1994).

The DSMC technique instructs particles to move and collide using kinetic-theory considerations that can capture the non-equilibrium gas behavior accurately. DSMC considers molecular collisions using stochastic rather than deterministic procedures over a time step which is a small fraction of the mean collision time, and each DSMC particle represents a large number of real gas molecules. The decoupling of particle ballistic motion and particle collisions improves the computational efficiency of DSMC greatly in comparison with other particle methods such as molecular dynamics (MD). The computational domain is divided into either a structured or unstructured grid of cells, with each cell of a dimension that is a small fraction of the local mean free path size. The cells are then utilized to select particles for collisions on a probabilistic basis, and they are also used for sampling the macroscopic flow properties. Intermolecular collisions are handled probabilistically using phenomenological models which are designed to reproduce real fluid behavior when the flow is examined at the macroscopic level. The DSMC technique has been shown to provide a solution to the Boltzmann equation as the number of simulated particles tends toward the true value within the flow field (Wagner, 1992). The DSMC approach is currently the dominant numerical method for rarefied gas flow applications.

In the DSMC methodology, particle clusters must be endowed with the correct properties to capture kinetic and rotational modes of energy storage. Vibrational excitation of the gas molecules as well as dissociation of both oxygen and nitrogen are likely to be important features of the flow around any hypersonic vehicle at the highest altitudes (80-120 km) and speeds, while, even at lower speeds and altitudes, vibrational excitation and limited dissociation of oxygen are still likely to be important (Anderson, 2006). Such real-gas effects need to be properly accounted for. In the present work, the quantum kinetic (Q-K) chemistry model is used to perform chemically reactive gas flow over the SARA capsule. This model describe the chemical reactions in a 5-species air model based solely on microscopic gas considerations (Bird, 2011; Gallis *et al.*, 2009; Bird, 2008; Wysong *et al.*, 2012; Scanlon *et al.*, 2015). The vibrational energy mode plays a key role in chemical reactions in the Q-K model. The vibrational modes of a gas are normally active when the system is sufficiently energised, e.g., under the high enthalpy conditions combined with shock structures commonly found in hypersonic applications. The vibrational mode forms part of the total energy budget and limits the amount of post-collision energy available to the translational and rotational modes. In addition, it often introduces a new mode of non-equilibrium to a rarefied gas system as the number of collisions required for vibrational relaxation is significantly higher than that for translational or rotational equilibrium (Gallis *et al.*, 2009). The full set of chemical reactions and its implementation into the dsmcFoam code is described by Scanlon *et al.* (2015).

The Q-K chemistry model was successfully implemented into the dsmcFoam code (Scanlon *et al.*, 2015) which take into account 19 reactions. In addition, Liechty and Lewis (2011) extended the Quantum-Kinetic model to include reactions involving charged species. In order to investigate the plasma formation around the SARA capsule, a 11 species reactions model (N_2, O_2, NO, N, O, N_2+, O_2+, NO+, N+, O+, e-) was implemented into the dsmcFoam as an extension of the 5 species reactions model. With this new set of chemical reactions, it is possible to investigate, in a more accurate manner, the reentry of space vehicle and to study the communication blackout caused by the electron layer formed around the spacecraft. In this way, the chemical reaction framework is modified to account for reactions involving charged particles and electrons, following the work of Liechty (Liechty, 2013). Currently, 116 reactions are implemented into the dsmcFoam code using the 11-species chemistry model. Some of these reactions are presented in Tables 1- 3.

Table 1: Molecule-Electron Ionization.

N^o	Reaction
1	$N_2 + e^- \rightarrow N_2^+ + e^- + e^-$
2	$O_2 + e^- \rightarrow O_2^+ + e^- + e^-$
3	$NO + e^- \rightarrow NO^+ + e^- + e^-$

Table 2: Atom-Electron Ionization.

N^o	Reaction
4	$N + e^- \rightarrow N^+ + e^- + e^-$
5	$O + e^- \rightarrow O^+ + e^- + e^-$

Table 3: Atom-Molecule Ionization.

N^o	Reaction
6	$N + N_2 \rightarrow N^+ + e^- + N_2$
7	$N + O_2 \rightarrow N^+ + e^- + O_2$
8	$N + NO \rightarrow N^+ + e^- + NO$
9	$O + N_2 \rightarrow O^+ + e^- + N_2$
10	$O + O_2 \rightarrow O^+ + e^- + O_2$
11	$O + NO \rightarrow O^+ + e^- + NO$

3. GEOMETRY DEFINITION AND FREESTREAM CONDITIONS

A detailed representation of the Brazilian Reentry Satellite is shown in Fig. 1. SARA was designed based on the cone-sphere configuration in which the nose radius (R_n) is 0.2678 m and 11.4° half-angle conical afterbody. The total length of the capsule is 1.410 m with a base radius of 0.5035 m. All the simulations were performed at 0° angle of attack, i.e., the incoming freestream is parallel to the x-axis.

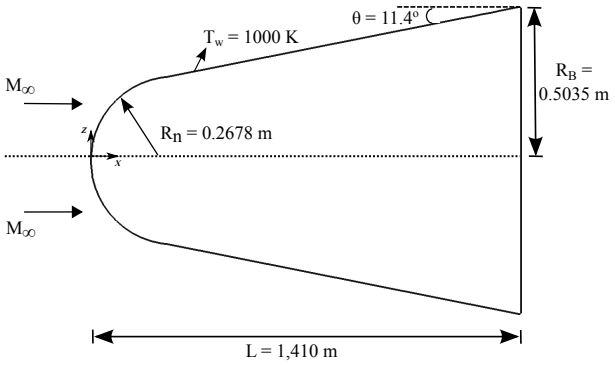

Figure 1: Schematic view of the SARA capsule.

The freestream conditions used in the present investigation correspond to those experienced by the Brazilian reentry capsule at 80 km altitude. In order to run the simulations, the freestream conditions were extracted from the U.S. Standard Atmosphere tables (NOAA/NASA/USAF, 1976). The freestream conditions for the altitude considered in this investigation are shown Table. 4.

At 80 km altitude, the atmosphere is composed by 78.68% N_2, 20.97% O_2, and 0.35% O. The freestream mean free path, λ_∞, is 4.67x10^{-3} m and it was determined using the variable hard sphere molecular model (Bird, 1994). The overall Knudsen number, Kn, is defined as the ratio of the molecular mean free path to a certain characteristic dimension. Considering the SARA's nose radius as the characteristic dimension, the Knudsen number correspond to 0.0174 and lies in the transition regime. The reentry velocity is set at 7860 m/s for the dsmcFoam computations and established based on the velocity-altitude-map presented by Pessoa Filho (2008).

Table 4: Freestream conditions experienced by the SARA capsule at 80 km altitude.

Parameters	U_∞ [m/s]	T_∞ [K]	n_∞ [m^{-3}]	ρ_∞ [kg/m^3]	p_∞ [Pa]	λ_∞ [m]
Values	7860	188.64	3.36×10^{20}	1.85×10^{-5}	0.105×10^{-1}	4.67x10^{-3}

4. COMPUTATIONAL DOMAIN AND BOUNDARY CONDITIONS

In the present investigation, advantage is taken from SARA's axisymmetry in order to reduce the computational costs. As shown in Fig. 2, the undisturbed freestream conditions is imposed -0.2 m upstream (X_u) of the SARA stagnation point, and the computational domain normal to the probe extended to a distance of 0.8 m in the $y-$ and $z-$directions. In the present investigation, the wake region was not considered and the computational domain is truncate at X_L = 1.41 m. The schematic of the computational domain and its main parameters is depicted in Fig. 2a).

After the generation of the cubic mesh and the definition of the boundary conditions, the OpenFOAM mesh utility called $snappyHexMesh$ is used to 'snap' the mesh on to the SARA CAD geometry growing hexahedral cells over the surface. A total of 14.1 million cells are used in the dsmcFoam calculations. The computational mesh employed in the present calculations is showed in Fig. 2b). The computational mesh is filled with 160.3 million DSMC particles. Freestream conditions are applied at the inlet of the computational domain. The flow at the downstream outflow boundary is supersonic and vacuum conditions are specified (Bird, 1994). The two perpendicular planes on the side of the capsule represents the symmetry planes, where all flow gradients normal to the plane are zero. At the molecular level, this boundary condition is equivalent to a specular reflecting wall. The wall temperature was kept constant at 1000 K and gas-surface interactions were modelled using diffuse reflections with full thermal and momentum accommodation.

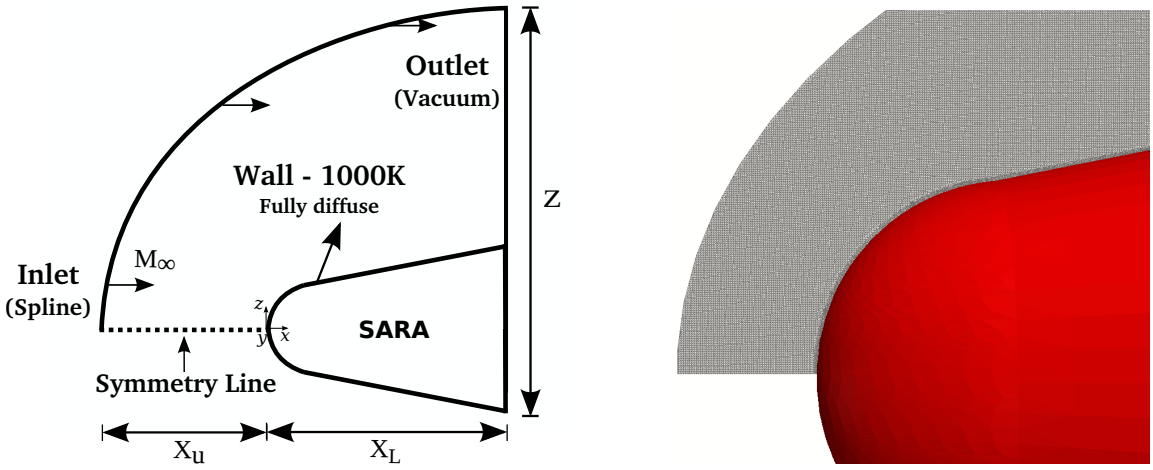

Figure 2: a) Computational boundary conditions and b) amplified view of the computational mesh at the SARA's nose.

5. COMPUTATIONAL RESULTS AND DISCUSSIONS

In this section, the primary macroscopic properties such as temperature, number density, pressure and velocity along the stagnation streamline are presented for rarefied hypersonic flows over the SARA capsule at 80 km altitude. The results are showed in nondimensional form, i.e, the macroscopic properties and the stagnation streamline are normalised by the freestream properties and stagnation streamline length, respectively.

In the DSMC calculations, translational, rotational and vibrational temperatures are obtained for each cell in the computational domain through the following equations,

$$T_{tra} = \frac{1}{3k_B}\overline{m\mathbf{c'}^2} = \frac{1}{3k_B}\frac{\sum_{j=1}^{N} m_j \mathbf{c'}^2}{N}, \tag{1}$$

$$T_{rot} = \frac{2m\varepsilon_{rot}}{k_B\zeta_{rot}} = \frac{2}{k_B\zeta_{rot}}\frac{\sum_{j=1}^{N} (\varepsilon_{rot})_j}{N}, \tag{2}$$

$$T_{vib} = \frac{\Theta_{vib}}{ln\left(1+\frac{k_B\Theta_{vib}}{\overline{\varepsilon}_{vib}}\right)} = \frac{\Theta_{vib}}{ln\left(1+\frac{k_B\Theta_{vib}}{\sum_{j=1}^{N}(\varepsilon_{vib})_j}\right)} \tag{3}$$

where k_B represents the Boltzmann constant, $\overline{\varepsilon}_{rot}$ and $\overline{\varepsilon}_{vib}$ are average rotational and vibrational energies per particle computed within the respective cell, and Θ_{vib} the characteristic vibrational temperature.

The effects of chemical reactions on the temperature distribution along the stagnation streamline are shown in Figure 3a). In this plot, the normalised temperature (T/T_∞) stands for the translational temperature (T_{tra}), rotational temperature (T_{rot}), vibrational temperature (T_{vib}). In addition, empty and full symbols represents inert and reactive gas flows, respectively.

According to Figure 3a), it is clearly seen that thermodynamic non-equilibrium occurs outside the cavities, as shown by the lack of equilibrium between the translational and internal kinetic temperatures. Thermal nonequilibrium occurs when the temperatures associated with the translational, rotational, and vibrational modes of a polyatomic gas are different. In addition, it is noticed a significant reduction on the peak of temperature when the chemical reactions are activated. For translational, rotational and vibrational temperatures the reduction on the peak temperature was 74,1%, 58,3% and 33,4%, respectively. The reduction on the peak temperature when chemical reactions are used for aerothermodynamics calculations of reentry vehicles demonstrates the importance of such code feature which have a significant impact on prediction of thermal protection system thickness and shock wave structure.

The shock wave thickness may be calculated as the distance between two points in the translational temperature plot located at half of the peak value. For the inert gas case, the shock wave thickness range from X = 0.025 to X = 0.265. However, in the dsmFoam-QK calculation, a reduction on the shock wave thickness is observed and it varied from X = 0,05 to X = 0,23. In this way, the strong shock wave formed upstream of the vehicle during the reentry was strong enough to activate the chemical reactions and promote a reduction of 25% on the shock wave thickness. The chemical reactions are mainly endothermic, i.e, they remove energy from the flow causing a reduction on the shock wave temperature and thickness. This result is clearly seen at the temperature distribution around the SARA capsule at Figures 4a) and b).

The density within the computational cells on the $dsmcFoam$ code is obtained using the following expression,

$$\rho = n\overline{m} = \frac{\overline{N}F_N}{V_c} = \frac{\sum_{j=1}^{N} m_j}{N}, \tag{4}$$

where n is the local number density, m is the molecular mass, and $\overline{N}$ and N are, respectively, the average and total number of simulated particles within a given cell. Furthermore, F_N represents any number of real particles and V_c is the computational cell volume.

The influence of chemical reactions on the number density distribution along the stagnation streamline is depicted on Figure 3b). From this plot, it is noticed that the number density far from the SARA capsule are similar for reacting and non-reacting flows. However, as the flow moves towards the vehicle, the number density increases at X = 1.025 and reaches the maximum value at X = 0.0. At the stagnation point, it is clear notice that the number density for reactive gas is higher than that presented for inert gas. Due the chemical reactions, new gas species are produced inside the shock contributing to an increase of 73% on number density at the stagnation region. The number density contours are shown in Figures 4c) and d).

The pressure determined by the $dsmcFoam$ code is obtained using the following expression,

$$p = \frac{1}{3}nm\overline{\mathbf{c'}^2} = \frac{1}{3}\frac{\overline{N}F_N}{V_c}\frac{\sum_{j=1}^{N} m_j \mathbf{c'}^2}{N}, \tag{5}$$

where n is the local number density, m is the molecular mass, $\mathbf{c'}$ is the thermal velocity, $\overline{N}$ and N are, respectively, the average and total number of simulated particles within a given cell, and V_c is the computational cell volume.

In a similar approach, the pressure distribution along the stagnation streamline is shown in Figure 3c). There is no significant changes on the pressure distribution up to location X = 0.3. Due the shock wave upstream of the vehicle, it is

observed a slight shift on the pressure profile from X = 0.3 to X = 0.075 in which reactive flow presented lower values. At the stagnation point, the pressure for reactive and inert gas reached is 1100 times the freestream pressure and no significant variations are observed at this region. The same physical behaviour is clear seen on the pressure contours in Figures 4e) and f).

The DSMC method is essentially a statistical method. In this way, the macroscopic properties are computed as averages from the microscopic properties in each cell in the computational domain. As a result, the velocity vector is given by the following expression,

$$\mathbf{c}_0 = \frac{\overline{m\mathbf{c}}}{\overline{m}} = \frac{\sum_{j=1}^{N} m_j \mathbf{c}_j}{\sum_{j=1}^{N} m_j}, \tag{6}$$

where m and $\mathbf{c}$ represents the mass and the velocity vector of each individual particle, and N is the total number of simulated particles within a cell.

According to Figure 3d), the velocity for reactive and non-reactive gas flow are similar up to location X = 0.475. From X = 0.475 to X = 0.1, similar trend to those observed for the pressure distribution along the stagnation streamline is observed, i.e, a shift on the velocity profile. At the stagnation point, the velocity is reduced almost to zero and no significant changes are observed. Figures 4g) and g) shows the velocity contours for reacting and non-reacting flow. From these contours, it is noticed that the velocity is not influenced by the chemical reactions apart from a very small region at the shock wave formed in front of the capsule.

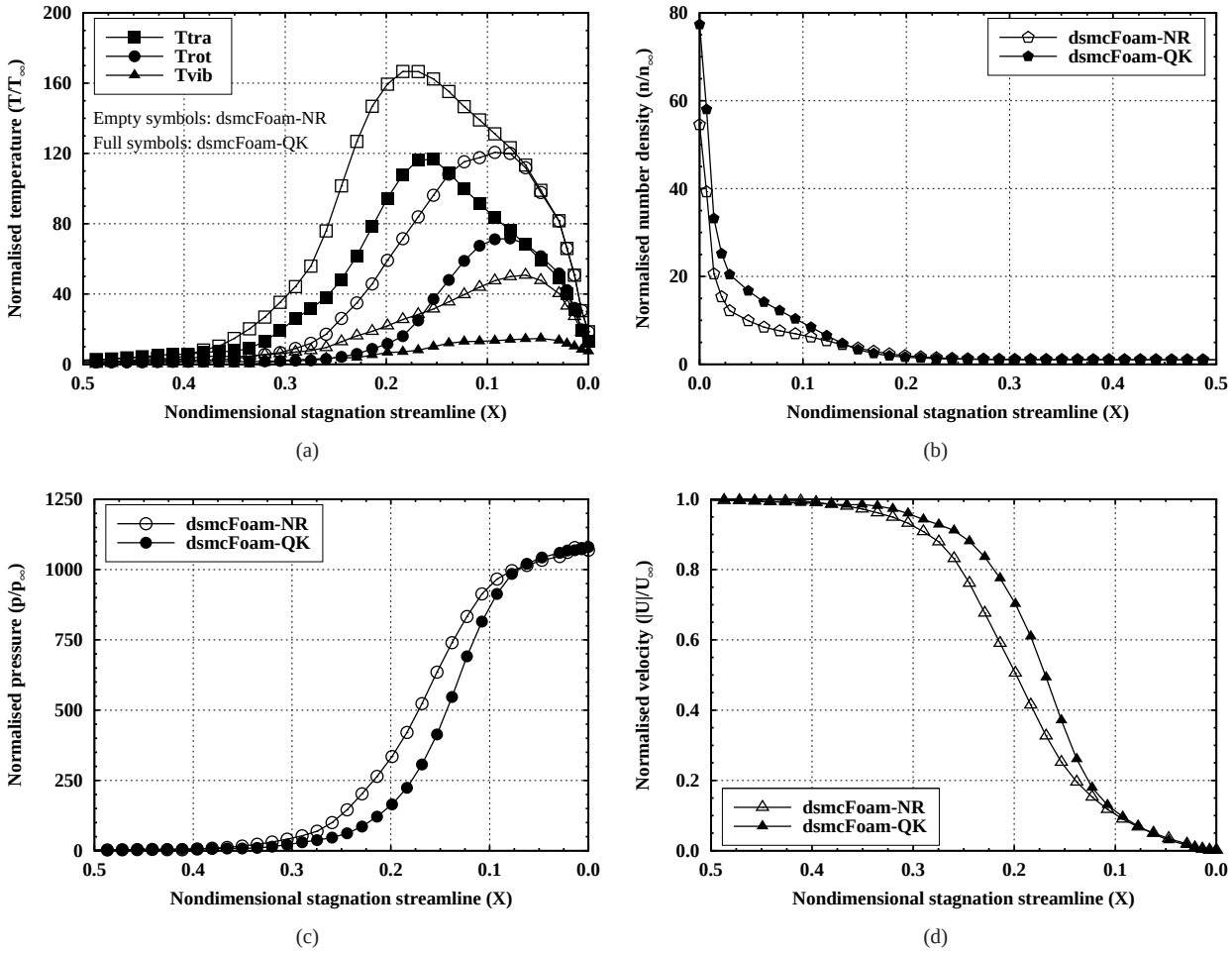

Figure 3: Normalised properties distribution along the stagnation streamline: a) temperature (T/T_∞), b) number density (n/n_∞), c) pressure (p/p_∞) and d) velocity ($|U|/U_\infty$). Empty symbols and full symbols represents inert (dsmcFoam-NR) e reactive (dsmcFoam-QK) gas flows, respectively.

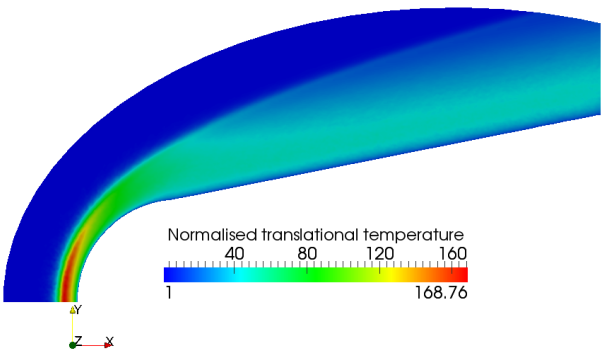

(a)

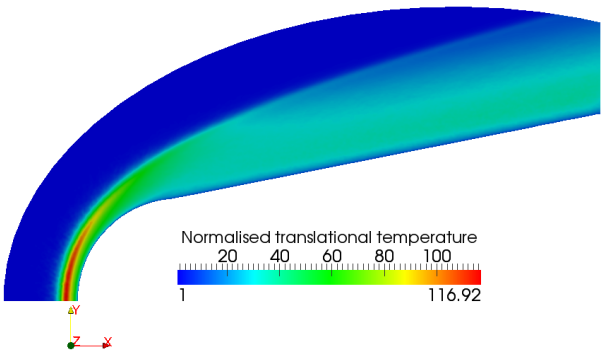

(b)

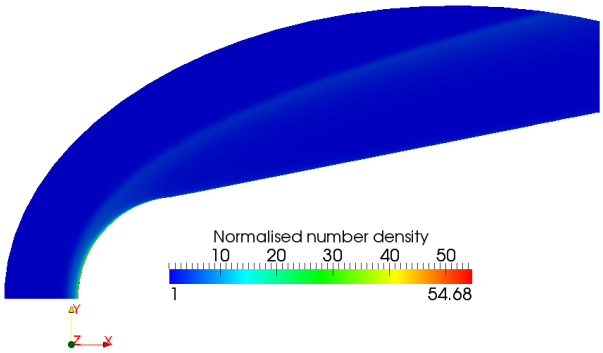

(c)

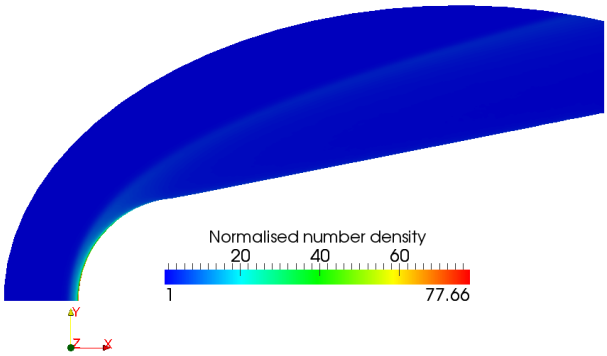

(d)

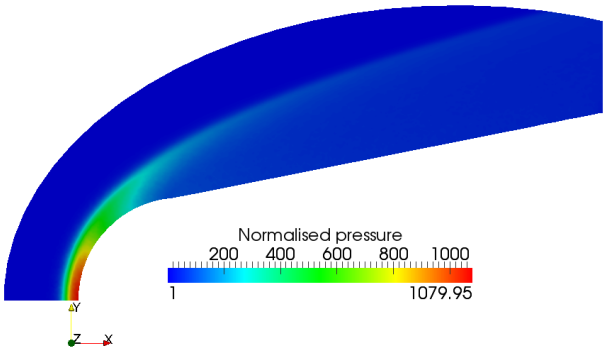

(e)

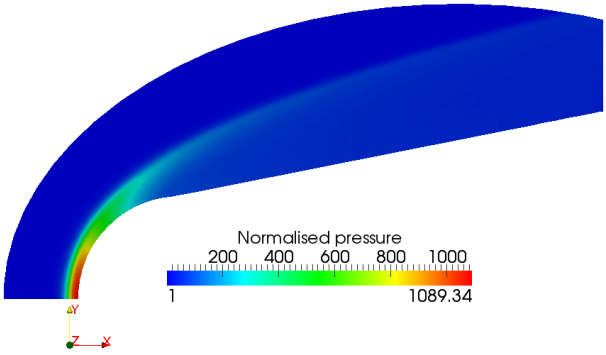

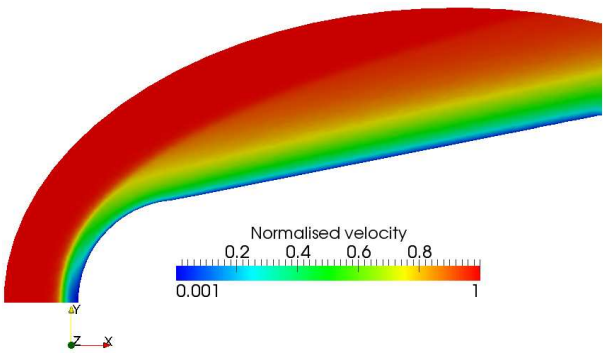

(g)

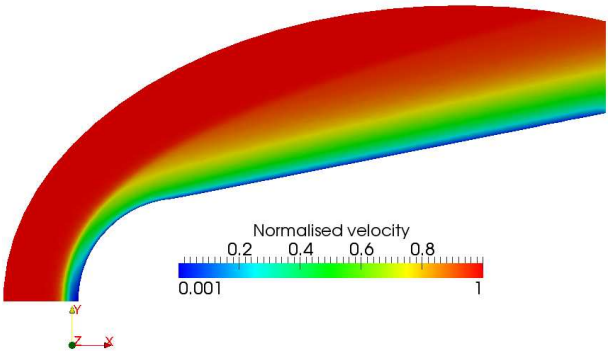

(h)

Figure 4: Primary properties contours over the SARA computational domain at 80 km altitude.

6. CONCLUDING REMARKS

Hypersonic rarefied flow simulations over the SARA capsule is performed using the direct simulation Monte Carlo method. The reactive gas flow is modeled employing the "Quantum Kinetic" chemistry model which takes into account an 11-species chemistry model and is able to perform 116 chemical reactions.

The analysis of the computational results shows that chemical reactions have a significant impact on the primary properties distribution along the stagnation streamline. From the primary properties the most affected was the temperature. There was a reduction of 74,1% on the translational temperature when the simulations were performed with chemical reactions. The temperature reduction inside the shock lead to a reduction on the shock wave thickness due the energy absorbed by the molecules to promote the chemical reactions. In addition, the production of species inside the shock by the chemical reactions increased by 73.3% the number density at the stagnation point. Finally, for the pressure and velocity distribution along the stagnation streamline, there was a slightly shift on the curves inside the shock region. However, no significant influence was observed in the pressure and velocity.

7. ACKNOWLEDGEMENTS

The authors gratefully acknowledge the support provided by CAPES via the PNPD program which allowed the development of this investigation. The authors also gratefully acknowledge the partial support for this research provided by Conselho Nacional de Desenvolvimento Científico e Tecnológico, CNPq, under the Research Grants No. 309985/2013-7, No. 400844/2014-1 and No. 443839/2014-0. The authors are also indebted to the partial financial support received from Fundação de Amparo à Pesquisa do Estado de São Paulo, FAPESP, under the Research Grants No. 2013/07375-0 and No. 2014/25438-1. The results were obtained using the dsmcFoam codes developed by the James Weir Fluids Laboratory based at the University of Strathclyde.

8. REFERENCES

Anderson, J.D., 2006. *Hypersonic and High Temperature Gas Dynamics*. McGraw-Hill.

Bertin, J.J. and Cummings, R.M., 2006. "Critical hypersonic aerothermodynamic phenomena". *Annual Review of Fluid Mechanics*, Vol. 38, pp. 129–157.

Bird, G.A., 2008. "A comparison of collision energy-based and temperature-based procedures in DSMC". In *26th International Symposium on Rarified Gas Dynamics*. Kyoto, Japan, Vol. 1084, pp. 245–250.

Bird, G.A., 2011. "The QK model for gas-phase chemical reaction rates". *Physics of Fluids*, Vol. 23, No. 10, pp. 1–13.

Bird, G., 1994. *Molecular Gas Dynamics and the Direct Simulation of Gas Flows*. Clarendon, Oxford.

Gallis, M.A., Bond, R.B. and Torczynski, J., 2009. "A kinetic-theory approach for computing chemical-reaction rates in upper-atmosphere hypersonic flows". *Journal of Chemical Physics*, Vol. 138, No. 124311.

Guzzo, F.R. and Azevedo, J.L.F., 2010. "A new particle-like method for high-speed flows with chemical non-equilibrium". *Journal od Aerospace Technology and Management*, Vol. 2, No. 1, pp. 17–32.

Liechty, D., 2013. *Extension of a kinetic approach to chemical reactions to electronic energy levels and reactions involving charged species with application to DSMC simulations,*. Ph.D. thesis, University of Maryland.

Liechty, D. and Lewis, M., 2011. "Extension of a kinetict heory approach for computing chemical reaction rates to reactions with charged particles". In *AIP Conference Proceedings*. Vol. 1333, pp. 1239–1244.

Machado, H.A., 2012. "Two-dimensional simulation of ablation due to aerodynamic heating in the SARA sub-obital platform". *High Temperatures - High Pressures*, Vol. 41, No. 4, p. 255.

Mather, D., Pasqual, J., Sillence, J. and Lewis, P., 2005. "Radio frequency (RF) blackout during hypersonic reentry". In *AIAA/CIRA 13th International Space Planes and Hypersonics Systems and Technologies*. Capua, Italy.

MCTI-AEB, 2012. "PNAE - Programa Nacional de Atividades Espaciais 2012-2021".

Morgenstern, A. and Moraes Jr., P., 2003. "Base flow investigation of a recoverable orbital capsule". In *41st Aerospace Science Meeting and Exhibit*. Reno, NV, AIAA Paper 2003-1252.

NOAA/NASA/USAF, 1976. "U. S. Standard Atmosphere". U.S. Government Printing Office.

Palharini, R.C. and Azevedo, J.L.F., 2017. "Thermochemical nonequilibrium computations of a Brazilian reentry satellite". *Journal of Spacecraft and Rockets*, Vol. 54, No. 4, pp. 961–967.

Pessoa Filho, J.B., 2008. "Velocity-altitude map for SARA capsule". Private Communication.

Santos, W.F.N., 2013. "Gas-surface interactions impact on the aerodynamic heating of a reentry Brazilian capsule". In *22nd International Congress of Mechanical Engineering*. Ribeirão Preto.

Scanlon, T.J., White, C., Borg, M.K., Palharini, R.C., Farbar, E., Boyd, I.D., Reese, J.M. and Brown, R.E., 2015. "Open-source direct simulation Monte Carlo chemistry modeling for hypersonic flows". *AIAA Journal*, Vol. 53, No. 6, pp. 1670–1680.

Wagner, W.A., 1992. "A convergence proof for Bird's direct simulation Monte Carlo method for the Boltzmann equation". *Journal of Statistical Physics*, Vol. 66, pp. 1011–1044.

Wysong, I., Gimelshein, S., Gimelshein, N., McKeon, W. and Esposito, F., 2012. "Reaction cross sections for two direct simulation Monte Carlo models: Accuracy and sensitivity analysis". *Physics of Fluids*, Vol. 24, pp. 1–15.

9. RESPONSIBILITY NOTICE

The authors are solely responsible for the printed material included in this paper.